Acta Biomaterialia 134 (2021) 348–356

Contents lists available at ScienceDirect

Acta Biomaterialia

journal homepage: www.elsevier.com/locate/actbio

Full length article

What do cells regulate in soft tissues on short time scales?

Jonas F. Eichinger[a,b,*], Daniel Paukner[b,c], Roland C. Aydin[c], Wolfgang A. Wall[a], Jay D. Humphrey[d], Christian J. Cyron[b,c]

[a] Institute for Computational Mechanics, Technical University of Munich, Boltzmannstrasse 15, 85748, Garching, Germany
[b] Institute for Continuum and Material Mechanics, Hamburg University of Technology, Eissendorfer Str. 42, 21073, Hamburg, Germany
[c] Institute of Material Systems Modeling, Helmholtz-Zentrum Hereon, Max-Planck-Strasse 1, 21502, Geesthacht, Germany
[d] Department of Biomedical Engineering, Yale University, 55 Prospect Street, New Haven, CT 06520, USA

ARTICLE INFO

Article history:
Received 9 April 2021
Revised 15 July 2021
Accepted 22 July 2021
Available online 28 July 2021

Keywords:
Homeostasis
Mechanosensing
Mechanoregulation
Cell-matrix interactions
Discrete fiber model

ABSTRACT

Cells within living soft biological tissues seem to promote the maintenance of a mechanical state within a defined range near a so-called set-point. This mechanobiological process is often referred to as mechanical homeostasis. During this process, cells interact with the fibers of the surrounding extracellular matrix (ECM). It remains poorly understood, however, what individual cells actually regulate during these interactions, and how these micromechanical regulations are translated to the tissue-level to lead to what we observe as biomaterial properties. Herein, we examine this question by a combination of experiments, theoretical analysis, and computational modeling. We demonstrate that on short time scales (hours) - during which deposition and degradation of ECM fibers can largely be neglected - cells appear to not regulate the stress / strain in the ECM or their own shape, but rather only the contractile forces that they exert on the surrounding ECM.

Statement of significance

Cells in soft biological tissues sense and regulate the mechanical state of the extracellular matrix to ensure structural integrity and functionality. This so-called mechanical homeostasis plays an important role in the natural history of various diseases such as aneurysms in the cardiovascular system or cancer. Yet, it remains poorly understood to date which target quantity cells regulate on the mircroscale and how it translates to the macroscale. In this paper, we combine experiments, computer simulations, and theoretical analysis to compare different hypotheses about this target quantity. This allows us to identify a likely candidate for it at least on short time scales and in the simplified environment of tissue equivalents.

1. Introduction

While many engineering materials remain stress-free, or in their respective production-induced stress state, in the absence of external loading, living soft tissues generally seek to establish a preferred mechanical state that is not stress-free. This state is often referred to as *homeostatic*. Notwithstanding this near steady state, cells are yet highly active. They constantly probe and transduce environmental cues into intracellular signaling pathways (mechanosensing) and adjust their interactions with the surrounding tissue fibers (mechanoregulation) accordingly [1–7]. To this end, cells use transmembrane receptors such as integrins to connect the intracellular cytoskeleton to fibers of the extracellular matrix (ECM). This unique dynamic regulatory system allows cells to establish and maintain a preferred mechanical state via a process that is often referred to as *tensional* [8] or *mechanical* [9] *homeostasis*. Compromised or lost mechanical homeostasis, and its underlying mechanosensitive and mechanoregulatory processes, are linked to some of the most predominant causes of death, including aneurysms [10–13] or cancer [14–19] on the organ scale, and

* Corresponding author.
E-mail addresses: eichinger@lnm.mw.tum.de (J.F. Eichinger), daniel.paukner@hereon.de (D. Paukner), roland.aydin@hereon.de (R.C. Aydin), wall@lnm.mw.tum.de (W.A. Wall), jay.humphrey@yale.edu (J.D. Humphrey), christian.cyron@tuhh.de (C.J. Cyron).

https://doi.org/10.1016/j.actbio.2021.07.054

to altered cellular processes such as cell migration [20–23], differentiation [24–26], and even survival [27–30].

Despite the prominent role of mechanical homeostasis in various physiological and pathophysiological processes, it remains unclear which mechanical quantity is regulated on a tissue level. In simple constrained tissue equivalents, it has been hypothesized that this ubiquitous control may seek to develop and maintain a certain state of tension in the tissue. Although continuum metrics of stress, strain, and those derived from them are unlikely to be sensed directly by cells [31], such metrics can nevertheless be good surrogate markers sufficient for data analysis and computation [8,32–37]. To address this open question, experiments using tissue equivalents have attracted increasing attention over recent decades [38]. Tissue equivalents are simple model systems of living soft tissues that consist often of collagen fibers seeded with living cells. When fixed at their boundaries in an initially stress-free configuration, tissue equivalents exhibit a characteristic behavior observed in numerous independent studies [8,32–45]. First, they rapidly build up a certain level of internal tension (phase I). Second, this level of tension is maintained for a prolonged period (phase II). If this steady state is perturbed (e.g., by stretching or releasing the tissue equivalent slightly), cells seem to regulate their activity such that the tension in the gel is restored toward the value prior to the perturbation [8,32,33]. It remains unclear, however, whether this value is recovered within a range consistent with homeostasis, noting that “homeo” means similar to in contrast with “homo” which means the same as [46].

In general, different time scales are involved in mechanical homeostasis. On short time scales (minutes to hours), cells can adapt the forces they exert on the surrounding ECM. On longer time scales (several days to months), cells may additionally turnover the ECM, that is, inelastically reorganize its microstructure or deposit and degrade matrix fibers (growth and atrophy) [39,47–49]. This article focuses on short time scales, in which the regulation of cellular forces can be assumed to be the dominant mechanism of mechanical homeostasis. Not only different time scales, but also different spatial scales are involved. On the microscale, individual cells likely sense and regulate elementary quantities such as forces in or displacements of surrounding fibers [31]. By contrast, on the tissue scale, this cellular activity leads to changes of continuum mechanical quantities such as stress, strain, or stiffness.

In this paper, we consider the question of which mechanical quantity individual cells regulate on the microscale on short time scales (where growth and remodeling can largely be neglected), and how this behavior translates into changes of continuum mechanical quantities on the tissue level. We address this question by a combination of three tools. First, we performed biaxial tissue culture experiments with a custom-built bioreactor [33]. Second, we developed a simple theoretical mechanical analog model to understand the governing principles of our experimental observations. Third, we used a detailed computational model resolving cell-ECM interactions on the level of discrete cells and fibers [50] to validate the results of our theoretical analysis.

2. Material and methods

2.1. Experimental study

Device and experimental procedure

To study the evolution of cell-generated tension in cell-seeded collagen gels we used our custom-built biaxial bioreactor, previously described in [33]. Briefly, the device consists of a bath, two force transducers, and four motors (Fig. 1). The device is placed within a humidified incubator (NU-8520, NuAire) at 37°C and a CO_2 level of 5% to ensure appropriate culture conditions. Two highly sensitive force transducers (World Precision Instruments), one for each axis, measure generated forces in the gel in the range of $0–1mN$ over multiple hours with negligible drift. Four high resolution stepper motors (Advanced Micro Systems) precisely control complex biaxial loading conditions. The device is controlled by a custom-written LabView code. Due to their fragility, the gels were polymerized inside the device to avoid unnecessary movements. To this end, a 3D-printed cruciform mold, which yields a homogeneous stress field in the central region of the specimen, is placed in the middle of the bath of an already assembled device. The collagen solution including the cells is prepared as described below and then pipetted into the mold. The liquid solution evenly distributes within the mold and around porous inserts which are firmly attached to the force transducers. Due to the change in temperature (the collagen solution is prepared on ice) the initially liquid solution starts polymerizing, forming over $30–45min$ a gel connected to the transducers used to control the gel strain. Subsequently, the bath is immersed within $80ml$ of culture medium. At this point, the mold is removed allowing the gel to float freely in the culture medium. This marks the start of the experiment. After an initial stress-free phase of approximately $30–60min$, the cells start to generate tension within the gel which is measured by the force transducers through the deflection of cantilever beams. The initial gel has a width of $\sim 10mm$ in the arms, a thickness of $\sim 4mm$ and a length of $\sim 25mm$ (between the porous inserts). The initial stiffness of a gel in the small deformation regime is estimated using the above dimensions and a strain of 1% (strain rate $0.1\%/s$), resulting in a Young’s modulus of approximately $1kPa$. The same strain rate was applied in all the experiments described herein.

Preparation of tissue equivalents

Primary smooth muscle cells (SMCs) were isolated from 13–15 week old male C57BL/6 wild-type mouse aortas. Cells extracted from the medial layer of the descending, suprarenal, and infrarenal aorta (all having a mesoderm embryonic lineage [51]) were mixed and then expanded in culture. Cells were maintained in culture medium consisting of Dulbecco’s Modified Eagles’s Medium (DMEM) (Gibco, Life Technologies, D5796), 20% heat-inactivated fetal bovine serum (FBS) (Gibco, Life Technologies), and 1% penicillin-streptomycin (ThermoFisher) in an incubator at 37°C and 5% CO_2. After cell extraction, cells were grown in one well of a 6-well plate before being transferred to a T25 flask in passage 1 (P1). In P2 and P3, cells were grown in T75 flasks. Cells were passaged at $70-80\%$ confluence roughly every 6 days. Passages 4 and 5 were used in all experiments. Cells were starved in medium containing 2.0% FBS for $24h$ prior to the experiments to inhibit proliferation during the experiments.

SMC-seeded collagen gels were prepared on ice following a protocol slightly modified from [33]. Briefly, $1.428ml$ of $5x$ DMEM, $0.683ml$ of a $10x$ reconstitution buffer (0.1N NaOH and $20mM$ HEPES; Sigma), and $0.790ml$ of high concentration, type-I rat tail collagen ($8.22mg/ml$; Corning) were mixed with $4.1ml$ of experimental culture medium containing $3.5 \cdot 10^6$ SMCs for a total volume of $7.0ml$ of gel solution. This resulted in a collagen concentration of 1.0mg/ml and a cell density of 0.5×10^6 cells/ml. Variations in cell density and collagen concentration (the latter automatically associated with changes of stiffness and pore size [52,53]) change the level of the homeostatic plateau tension, but not the general observed behavior [33]. The experimental culture medium consisted of DMEM supplemented with 2.0% FBS and 1% penicillin-streptomycin. To avoid proliferation and to minimize parasitic effects of fluctuating concentrations of FBS components that naturally appear between batches, we used only 2% FSB in the experimental culture medium. The final gel solution was pipetted into a cruciform mold as described in the previous section. Subsequently, the experiment was started. During an experiment (which lasted

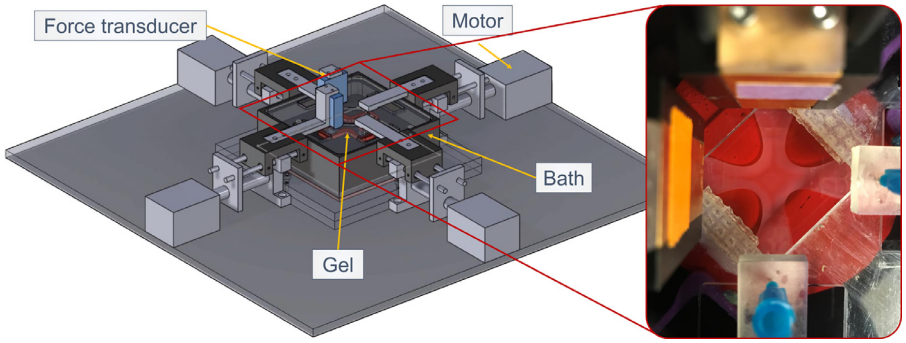

Fig. 1. Biaxial testing device for cell-seeded collagen gels as introduced in [33]: schematic drawing (left) and cruciform-shaped gel sample (right). The base plate upon which the system rests (left) is placed on a shelf within a custom incubator, with all wires exteriorized through a custom sealed port and connected to the power source or controlling computer.

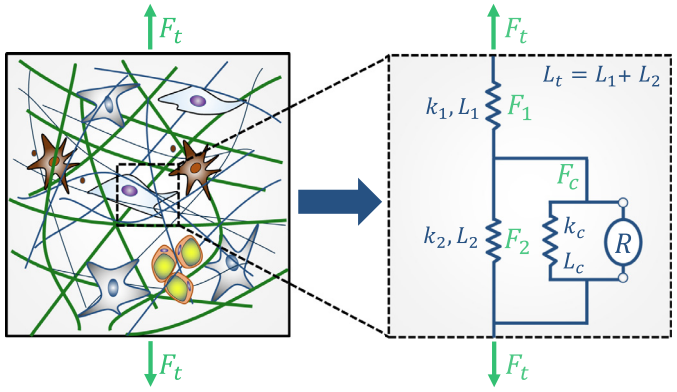

Fig. 2. Mechanical analog model of a three-dimensional fiber matrix with embedded cells: the sum of all cellular forces in the direction of interest is given by F_c composed of an active component mediated by the regulator element R and a passive component dictated by the spring constant k_c. In this way, cells pull on ECM fibers. These fibers are connected via the network to other fibers parallel to the cell (category 2), which are in general compressed when cells exert contractile forces. Both sets of fibers are represented by elastic springs. Displacements are fixed at the outer boundary of the system. The resulting force on the tissue level (as measured, for example, by force sensors at clamped boundaries) corresponds to the force F_t in the mechanical analog model. L_1, L_2, and L_t describe the lengths at deformed/homeostatic states reached by cellular contraction. Note, the analog model can also be understood as the smallest possible representative volume element (RVE) for soft tissues.

less than 48h), the medium was not changed to avoid disturbing the highly sensitive force measurements.

2.2. Mechanical analog model for soft tissue mechanical homeostasis on short time scales

To understand the underlying principles of mechanical homeostasis of soft tissues, we developed a simplified mechanical analog model (Fig. 2). The ECM, that is, the mechanical environment in which cells reside, was modeled as an elastic network of fibers. For simplicity, we focus only on a single direction, noting that an analogous discussion would be possible in any other direction. The scenario of a single direction leads to the mechanical analog model depicted in Fig. 2, consisting of two categories of fibers 1 and 2 and cells. Cells in vivo (and in vitro) attach to nearby matrix fibers via focal adhesions and then contract. This leads, in a connected fiber network, to fibers that are compressed (category 2, represented by elastic elements in parallel to cells in the analog model) and fibers that are stretched (category 1, represented by elastic elements in series to cells in the analog model). Note that this is true in any direction and can occur in several independent spatial directions at the same time in case of a multi-axial stress state. In general, the mechanical function of the fibers is represented by elastic spring elements. The forces in the spring elements (i.e., the forces transmitted through all fibers of category 1 and 2, respectively, with unit [N]) are denoted by F_1 and F_2. Cells are represented by an elastic spring (representing their passive stiffness) with a regulator element in parallel. The latter represents the active forces exerted by the stress fibers in the cytoskeleton on the surrounding ECM fibers. The force exerted by all cells in the direction of interest is denoted by F_c. It is composed of an active component exerted by the regulator element R and a passive component. Generally, the passive elastic forces of the different elements are characterized by the overall stiffness k_i and a length L_i in the direction of interest with $i \in \{1, 2, c\}$. That is, for the passive elastic parts of our model, changes of length and force are related by

$$\Delta F_i = k_i \Delta L_i, \quad i \in \{1, 2, c\}. \tag{1}$$

The overall force of the tissue (with length L_t) in the direction of interest is denoted by F_t. It is important to note that this model can also be interpreted as the smallest possible representative volume element (RVE) of a uniaxially loaded or constrained soft tissue. Viscoelastic effects were neglected because they manifest in the ECM on time scales much shorter than that for mechanical homeostasis.

2.3. Three-dimensional discrete fiber and cell model

Network model

To simulate soft tissue mechanics on the level of individual cells and fibers, we used the computational framework presented in [50] and shown Fig. 3. Briefly, we reconstructed periodic RVEs of fiber networks using stochastic optimization that neatly matched the crucial microstructural characteristics of actual collagen gels, that is, their valency, free fiber length, and orientation distributions. These descriptors are predominantly responsible for the mechanical properties of fibrous networks [54]. Individual fibers were discretized with nonlinear beam finite elements, which are well-known to capture the most important modes of the mechanical deformation of fibers, that is, axial tension, torsion, bending, and shear. Networks were formed by coupling both translational and rotational degrees of freedom at entanglement points of two fibers. Fibers were assumed to have circular cross-sections with a diameter of 180nm [55] and an elastic modulus of 1.1MPa [56] to mimic the collagen type-I fibers that were used in our experiments.

Cell adhesion model

Biologically, intracellular structures such as the actomyosin cytoskeleton are physically coupled to the surrounding ECM fibers via transmembrane integrins that cluster to form focal adhesions [4,7]. This coupling allows cells to receive mechanical cues from their environment and to react to them, for example, by adapting their contractility. We model cells as particles that can form elastic connections to predefined binding spots on nearby matrix fibers with a certain probability (Fig. 3). These connections represent the

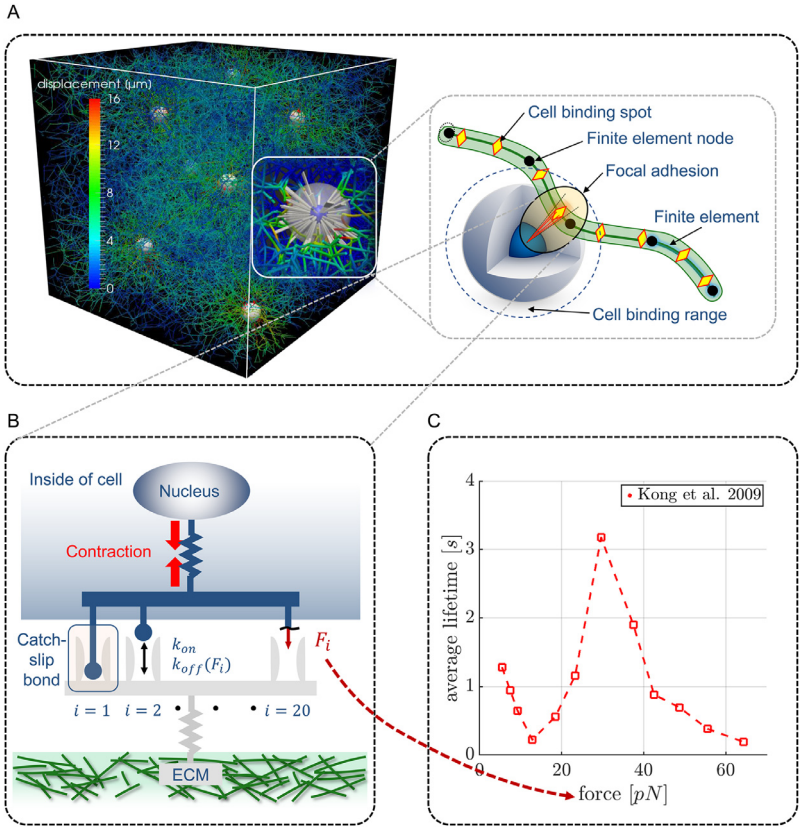

Fig. 3. (A) RVE of our three-dimensional discrete fiber and cell model. Fibers are modeled as nonlinear beam elements, on which cells can exert contractile forces via elastic links representing focal adhesions. (B) Each focal adhesion consists of up to 50 so-called integrin clusters, one of which is shown here, each formed by up to 20 integrins. We model each integrin cluster as being connected to one actin stress fiber. Integrins are modeled as molecular clutches, i.e., they bind and unbind according to specific binding kinetics. (C) [45] determined a catch-slip bond behavior for single integrins, which we model with a force-dependent lifetime for each bond matching this experimental data.

entire cell-matrix adhesion complex, consisting of the contractile cytoskeleton and the focal adhesions. The latter are modeled as multiple integrin clusters, each of which consists of 20 integrins (Fig. 3B). The on- and off-rates of the bonds between integrins and the ECM ligands were chosen to mimic their characteristic catch-slip bond behavior [57,58] (Fig. 3C), that is, a force-dependent lifetime of each integrin connection peaking at some preferred load state. Cell contractility was modeled by the contraction of established cell-ECM connections at a rate of $0.1 \mu m/s$ [59,60]. This increasing contraction automatically limits the lifetime of individual cell-ECM connections, which dissolve with increasing probability beyond a critical level of loading. Our model thereby captures typical lifetimes of focal adhesions on the order of minutes, while the turnover rate for most proteins involved in the adhesion complex is on the order of seconds. This implies that our model realistically describes the lifetime of focal adhesions as being determined by the interactions of many individual binding and unbinding events of integrins [61].

All simulations were performed using displacement-controlled boundary conditions for the considered RVEs, consistent with the experimental system. The entire computational framework was implemented in the in-house finite element code BACI [62].

3. Results

3.1. Experimental results

Experimental studies of cell-seeded collagen gels (tissue equivalents) subject to mechanical perturbations so far largely suffer from the unsatisfactory short periods over which the gels have been monitored after the perturbations (e.g., only 30 *min* in [8,32]). Therefore, it has remained unclear whether tissue equivalents recover the prior state of tension or only to some extent after perturbations. To close this gap, we performed our experiments with cruciform-shaped tissue equivalents (leading to uniaxially loaded arms and a biaxially loaded central region) over prolonged periods up to 40*h*. After 24*h* we strained some of the gels by 2% or −2%, respectively, allowing another 16*h* to observe possible recovery. Interestingly, the addition of Triton X after 40*h* to induce cell lysis led to a rapid decrease of the gel tension to zero (Fig. 4A inset). This implies that all forces measured were actively applied by the cells, with no inelastic change of the stress-free configuration of the matrix. Similar results were found before [44]. Because the turnover of collagen (i.e., deposition and degradation of collagen fibers by cells) typically happens on the time scale of 3+ days, it appears also justified to assume that mass turnover can most likely be neglected in our experiments [2,48,49,63,64].

In this setting, we initially observed the well-known increase of tension up to a homeostatic plateau [8,32,39–45]. Also as previously reported for porcine SMCs [65], this first stage was followed by a slight decline of tension (Fig. 4A). In cases where tissue equivalents were strained by a 2% step at 24*h*, gel tension first increased in a step-wise manner (elastic response of cells and matrix resulting in a step-like increase in F_t of $\sim 50\%$) followed by a period where tension decreased back toward the level prior to the perturbation (some isolated cellular response). However, even after 16*h*, the original level of tension was not fully recovered, but rather re-established within $\sim 10-15\%$ deviation from the prior value (Fig. 4B). Analogously, if the gels were released by 2% at 24*h*, one first observed a step-wise drop of tension (elastic response of cells

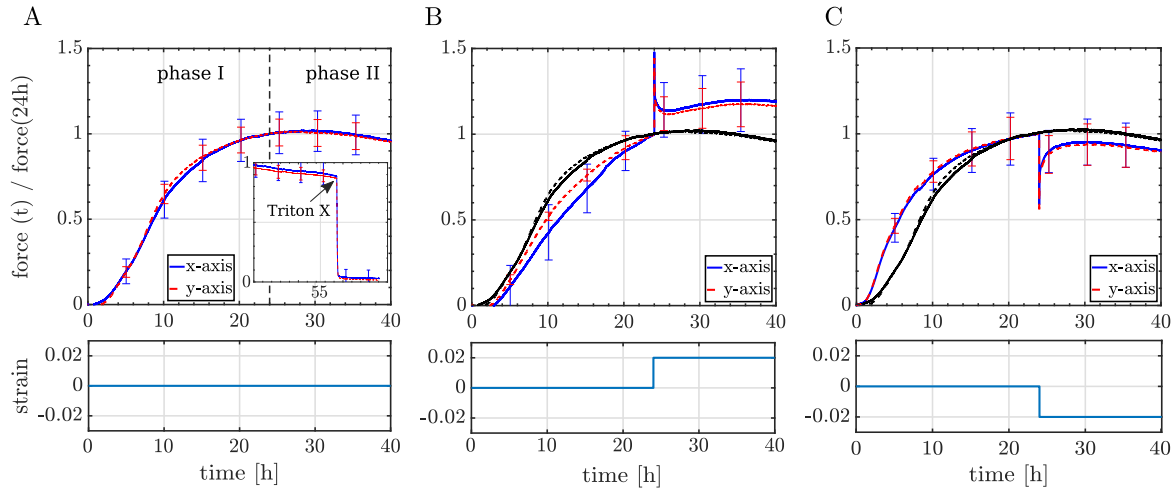

Fig. 4. Normalized force F_t at the outer boundary of cruciform-shaped collagen gels (arms of the gel aligned with x- and y-axis, respectively) seeded with primary aortic SMCs. Each curve shows the mean ± SEM of three identical experiments using a collagen concentration of $1.0 mg/ml$ and a cell density of $0.5 \cdot 10^6 cells/ml$. (A) Unperturbed tissue equivalents (normalized with $F_x(24h) = 720\mu N$ and $F_y(24h) = 729\mu N$) suggested a nearly isotropic biaxial response. (B) Tissue equivalents perturbed with an equibiaxial strain step of 2% at $24h$ (normalized with $F_x(24h) = 602\mu N$ and $F_y(24h) = 588\mu N$). (C) Tissue equivalents perturbed with an equibiaxial step-wise release by 2% at $24h$ (normalized with $F_x(24h) = 664\mu N$ and $F_y(24h) = 626\mu N$). Lines without error bars in (B) and (C) represent experiments without perturbation from (A), hence revealing some specimen-to-specimen variations.

and matrix resulting in a step-like decrease in F_t of $\sim 40\%$), followed by a period where tension increased back toward the level prior to the perturbation (some isolated cellular response). Again, however, even after $16h$ the original level of tension was not fully recovered (Fig. 4C), but rather re-established within $\sim 5-10\%$ deviation from the prior value.

It is worth mentioning that the presented data show a slight decrease of tension in phase II and therefore not an exact conservation of a specific tension. Such a behavior could arise for several reasons. First, a gradual slippage of the gel from the clamping mechanism could be responsible. We excluded this possible reason by pulling on the tested gels after the experiments with a higher force than during the experiments, which was not observed to result in any significant slippage. A second possible origin of the decline in tension is the low serum concentration of 2% that was used in the experimental medium. In preliminary studies, we confirmed that an increased serum concentration leads to higher tension. However, a decline of tension after approximately $24h$ was observed regardless of the serum concentration. Thus, the concentration of FBS in the experimental medium is presumably not responsible for the decline in tension in phase II. In [38], we compared the evolution of tension in constrained tissue equivalents across a large number of studies using a setup similar to ours. Different force generation patterns over time were observed (including decline of tension), depending on factors such as cell type, cell extraction method, and growth factors [38]. We therefore conclude that the slight decline of force is probably cell type specific. This assumption is supported by the study of [65], which reported a similar declining behavior for arterial SMCs. It is worth mentioning that free-floating collagen gels often exhibit a contractility persisting even beyond $48h$ [47,66]. Yet, the free-floating gel is a very different boundary value problem where the cells are not able to reach the same uniform (homeostatic) tension [66], and it is thus not suitable for a direct comparison with uni- or biaxially constrained gels.

3.2. Mechanical analog model

The primary observation of the previous section is: when cell-seeded tissue equivalents were perturbed from the apparent homeostatic state achieved over $24h$, they did not recover precisely F_t (over a period of $16h$). To understand the origin of this behavior, we employed the mechanical analog model introduced in Section 2. In this model, the external force on the tissue F_t needs to equal the elastic force F_1 in the tissue region under tension in series with the cells, which has to balance the sum of the cellular force F_c and the elastic forces F_2 in the tissue region under compression. This yields

$$F_t = F_1 = F_2 + F_c. \tag{2}$$

We now assume the system to be in a homeostatic state (Fig. 5A), in which the initially stress-free regions 1 and 2 were deformed by tensile cell forces $F_c > 0$. One can easily show that this results in an initial homeostatic force on the tissue level, in case of fixed displacements at the outer boundary, of

$$F_{t0} = \left(1 - \frac{k_2}{k_1 + k_2}\right) F_c. \tag{3}$$

We then subject the tissue to a step-wise stretch or release by a change of length ΔL_t (Fig. 5B). Keeping ΔL_t constant after the perturbation results in a permanent change of tissue length

$$\Delta L_t = \Delta L_1 + \Delta L_2. \tag{4}$$

The elastic response of the system will be a step-wise increase of F_t, the quantity that can be measured externally. The subsequent evolution of the forces in the tissue is directly governed by cellular mechanoregulation if we assume that the fiber network only deforms elastically (neither growth nor inelastic remodeling on the short time scales considered).

In the following, we discuss on the basis of our mechanical analog model competing hypotheses regarding the quantity that cells actually regulate. We discuss the observations on the macroscale that these hypotheses would yield and compare them with those in our experiments. It appears reasonable to assume that cells could possibly sense and thus regulate on the microscale three quantities (cf. also [31]): their shape (hypothesis I), the active force they exert through their focal adhesions (hypothesis II), or the strain of the fibers to which they are connected by focal adhesions (hypothesis III). This yields three hypotheses which will be discussed in the following. We assume for simplicity a linear-elastic behavior at the microscale, that is, deformation-independent stiffnesses k_i.

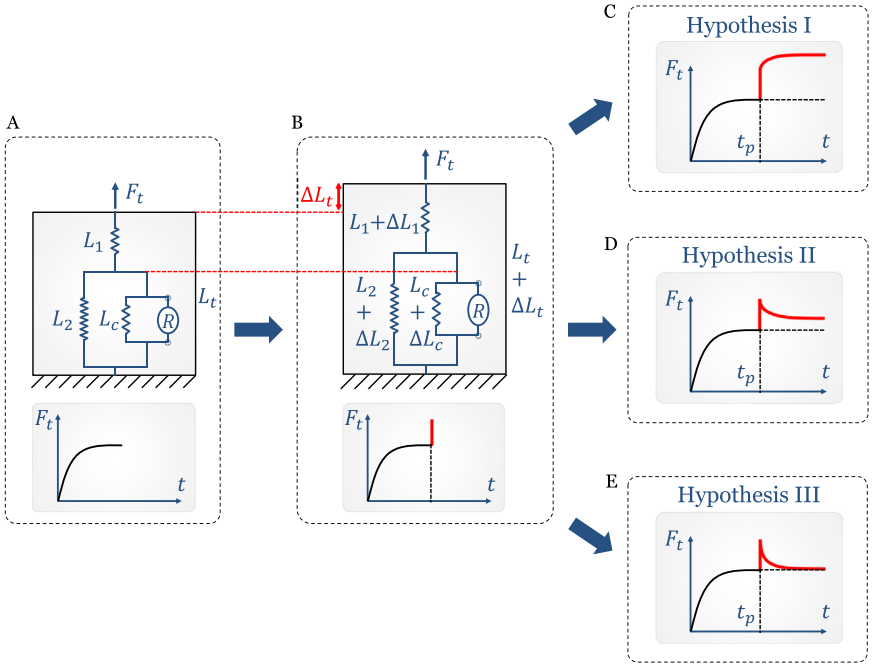

Fig. 5. Short-term response of the (A) mechanical analog model at steady state (after the force $F_c > 0$ built up over time) to a (B) strain step assuming different regulatory targets of an individual cell formulated in (C) hypothesis I (regulation of cell shape), (D) hypothesis II (regulation of contractile forces of cells on ECM), and (E) hypothesis III (regulation of tissue strain). Note that only hypothesis II agrees with experimental observations.

3.2.1. Hypothesis I: cells restore their shape

If cells restore their shape after perturbations, they restore L_c and thus also L_2 and F_2. To this end, cells have to contract after an initial step-wise stretch of the whole tissue and thus have to increase F_c. After regulation, $\Delta L_1 = \Delta L_t$ and with F_2 fully restored,

$$\Delta F_t = \Delta F_1 = \Delta F_c = k_1 \Delta L_1 = k_1 \Delta L_t. \tag{5}$$

Therefore, ΔF_t increases its magnitude compared to that after the perturbation, which is $|\Delta F_t| = |k_1(\Delta L_t - \Delta L_2)|$. This behavior is illustrated in (Fig. 5C), and is in contradiction to our experimental observations.

3.2.2. Hypothesis II: cells restore cellular forces

As discussed previously [38,58,67], cells have a tendency to build stable bonds to the ECM fibers only in a certain constant range of forces. Thus, we examine the response of our analog model if cells restore the cellular forces after perturbations, i.e., F_c. As Eq. (2) must hold also for changes of forces due to changes of lengths, we have, once F_c has been restored,

$$k_1 \Delta L_1 = \Delta F_1 = \Delta F_2 = k_2 \Delta L_2. \tag{6}$$

Combining Eqs. (1), (4), and (6) yields

$$\Delta F_t = \Delta F_1 = \Delta F_2 = \frac{k_1 k_2}{k_1 + k_2} \Delta L_t. \tag{7}$$

Thus, a restoration of F_c after the perturbation necessarily implies a permanent increased value of both F_2 and F_1 and thus also of F_t for $\Delta L_t > 0$, and a permanently decreased value for $\Delta L_t < 0$ (Fig. 5D). This is the behavior observed in our experiments.

Strikingly, this may suggest that most short-term tissue equivalent experiments do not study a regulation of the mechanical state of the ECM, but rather a superposition of the passive matrix response (according to Eq. (7) equal to the remaining offset) and the cellular regulation of a specific contractile force, which represents a relaxation (recovery) in case of extension (release) as an external mechanical perturbation. A direct quantitative comparison between experimental data and our analog model is presented in the supplementary material.

Therefore, our results agree with the findings of [67], which showed that isolated cells restore a specific cellular tensional state. Here we predict this in a three-dimensional fibrous, multi-cellular environment compared to a single cell on a two-dimensional substrate.

Moreover, the changes represented by Eq. (7) suggest a simple additional test of hypothesis II by future experiments. By performing the experiments shown herein in the future with two or more different fiber concentrations (implying different network stiffnesses [62,64,66]) and measuring the resulting residual offset ΔF_t, one could check whether the latter is in agreement with Eq. (7). If so, it should - ceteris paribus - increase by the same factor as the network stiffness.

3.2.3. Hypothesis III: cells restore strain in ECM fibers

If cells restore the strain in the ECM fibers on which they are pulling after the prescribed perturbations, they restore L_1 and thereby also F_1 and F_t. Thus, hypothesis III also contradicts our experiments, where F_t is not exactly restored after perturbations. To understand the problem of hypothesis III, note that it implies $\Delta L_2 = \Delta L_t$ in the long run (that is, after a step-wise elastic deformation and the subsequent mechanoregulation by the cells). It thus implies $\Delta F_2 = k_2 \Delta L_t$. With $0 = \Delta F_1 = \Delta F_2 + \Delta F_c$, one obtains

$$\Delta F_c = -\Delta F_2 = -k_2 \Delta L_t. \tag{8}$$

From this equation we see a possible reason why cells apparently do not restore the strain and thereby not exactly the tension in the fibers on which they are pulling. As apparent from Eq. (8), they would require information about the stiffness or forces in the region under compression. However, this would require that the cells not only sense the general stiffness of the surrounding tissue, but also specifically the extensional stiffness of the part of the ECM which they compress. Moreover, cells do not have information about ΔL_t. Thus, it appears that cells do not have the information necessary to regulate the strain of the fibers on which they pull, which explains why hypothesis III seems to be in disagreement with our experiments.

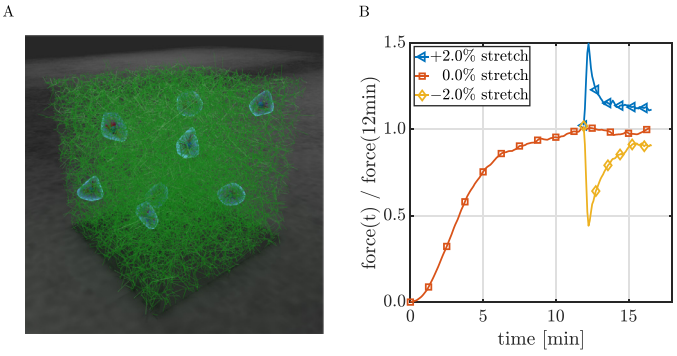

Fig. 6. (A) RVE simulated with a discrete fiber model; triaxial boundary conditions are applied to externally perturb the system. Cell shape is reconstructed around cell-matrix links using three-dimensional Delaunay triangulation. (B) Tissue tension in simulations initially increases to a plateau value. If this plateau value is perturbed, the prior level of tension is restored toward, but not precisely to, the prior steady state value, consistent with the concept of homeostasis now with a mechanistic understanding.

3.3. Discrete fiber network model

The main conclusion drawn from our experimental data and our simple mechanical analog model is: on short time scales, cells do not - and in fact cannot - control the tension in the tissue to a specific value. Cells only regulate the forces they exert on the surrounding fibers. This naturally leads to a residual offset in the tissue tension after perturbations on time scales too short for remodeling or de novo deposition and degradation of fibers. To corroborate this understanding of cellular mechanoregulation, we performed computer simulations with a discrete fiber-network model introduced in [50]. We studied an RVE with a covalently cross-linked fiber matrix (Fig. 6). The size, fiber concentration, and cell concentration of the simulated RVE were chosen to be equivalent to the cell and collagen density in our experiments.

Following [58], catch-slip bonds were assumed between cells and ECM fibers. These bonds are chemically the most enduring in a very specific regime of forces. Our objective was to test whether this behavior of the catch-slip bonds together with cellular contractility alone allows cells within the overall system to effectively control the forces they exert on the surrounding fibers [67] (i.e., F_c in our mechanical analog model), and whether this leads to a residual offset of the tissue tension after mechanical perturbations. As Fig. 6 reveals, this is indeed the case, confirming that the catch-slip bond is a key factor enabling cells to accurately control the contractile forces they exert on surrounding ECM fibers.

A notable difference between the simulation results in Fig. 6 and the experimental results in Fig. 4 is the time scale. In our simulations, mechanical homeostasis develops over a few minutes and thus matches well with experimental results of single cells on purely elastic substrates [67,68]. Yet, in our experiments the homeostatic state is established over many hours. A possible explanation for the difference in the time scale are viscoelastic effects that occur in the gel on the time scale of hours and are not included in the model. Another reason might be that gels increase their stiffness over time when placed in the incubator for multiple hours due to progressing polymerization. Possibly, also complex biochemical interactions between different cells could delay the homeostatic state, which is also not accounted for in the model.

4. Discussion and conclusions

A major shortcoming of previous studies about how tissue equivalents restore a preferred level of tension after an external perturbation (e.g., [8,32]) is the short period of less than an hour over which restoration of tension was monitored. Within such short periods, no new steady state of tension was re-established, leaving unanswered the question, within which tolerance the prior tension is restored after perturbations. This made it difficult to understand which mechanical target quantity is actually preserved by mechanical homeostasis. To overcome this problem, we used herein the device introduced in [33] to track the restoration of tension after perturbations over periods around 30 times longer than previous studies. These data formed the basis of a combined theoretical and computational analysis.

First, to unravel micromechanical principles underlying cellular mechanoregulation, we developed a mechanical analog model to test three competing hypotheses regarding what cells sense and regulate on the microscale. Hypothesis I assumed that cells regulate their own dimension. Hypothesis II, motivated by the experiments of [67], assumed that cells regulate the contractile forces they exert on the ECM. Hypothesis III assumed that cells regulate the strain in the surrounding tissue. Only hypothesis II was consistent with the observed behavior. We therefore conclude that it is likely that cells in gel-like tissue equivalents regulate only the forces they exert on the ECM (at least on short time scales), which by Newton's third law implies the forces that the ECM exerts on the cells, rather than any tissue-intrinsic quantity.

Using an advanced computational model resolving discrete fibers, cells, and their interactions, we confirmed that the catch-slip bond by which integrins connect cells and matrix fibers can endow cells with an ability to regulate the contractile forces they exert on the ECM. In general, catch-slip bonds differ from most chemical bonds in that their lifetime does not monotonically decrease with increasing mechanical load on the bond. There is rather a specific optimal loading at which the stability of these bonds attains a maximum [58]. In agreement with experiments [67], our studies reveal that this maximum determines the level at which cells can regulate the contractile forces they exert on ECM. It is worth noting that the computational studies with our discrete fiber model can support the assumption that the catch-slip bond is sufficient for cells to regulate the forces they exert on the ECM. Yet, these studies cannot prove that this is the only mechanism by which cells can or do act in this setting.

An important conclusion from both our mechanical analog model and simulations with our discrete fiber model is that the passive elasticity of the ECM acts in parallel with the cells to form an essential part of the mechanoregulatory system on the tissue level. Our findings suggest that the residual offset between the matrix tension before and after strain perturbations can be explained only from the passive elasticity of the ECM acting in parallel. To the authors' knowledge, this insight is new and can be used to design future experiments. To study mechanical homeostasis on the level of single cells, cells have been placed between an elastic cantilever and a rigid substrate (Fig. 7A, [69]), and on top of a stretchable micropost array (Fig. 7B, [67]). In both cases, the elastic effect of fibers acting in parallel with the contractile forces exerted by the cells is missing as illustrated in Fig. 7C. This means, neither of these systems mimic well that which defines mechanical homeostasis on the tissue scale. Hence, it will be essential to develop additional experimental set-ups that model the critically important cell-matrix interactions.

An important question for future work is, how can the conclusions drawn here be tested further by additional experiments. As discussed above, a simple test for our conclusion, that the contractile forces exerted by cells are the quantity controlled by the cells on short time scales at a tissue level, could be performed by running the experiments shown herein with several different collagen concentrations and observing whether the residual offset between the tissue tension before and after the perturbation scales with (approximately) the same factor as the tissue stiffness.

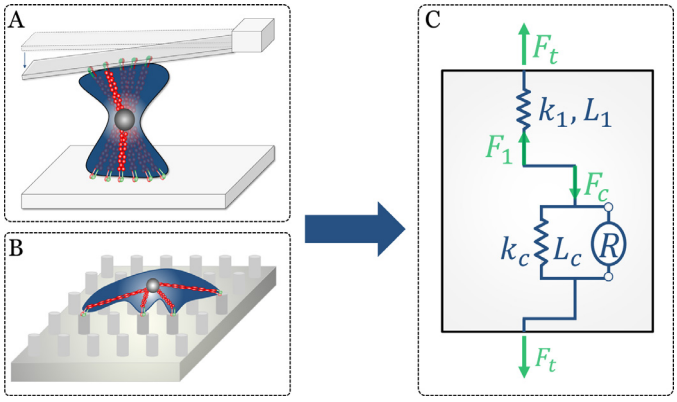

Fig. 7. Schematic drawing of experimental set-ups used by (A) [65] and (B) [46] to study mechanical homeostasis on the level of single cells. Both set-ups miss the elastic fibers acting in parallel to cells in real tissues and thus an important element defining how tissues respond to perturbations of their homeostatic state.

Another way to test these conclusions would be to perform a series of experiments with a varying cell density. While the residual offset between the matrix tension before and after a perturbation was shown in Eq. (7) to be independent of the contractile forces of the cells in the pre-perturbed state, Eq. (3) reveals that homeostatic tissue tension prior to the perturbation scales linearly with the magnitude of these forces. That is, findings herein predict a decreasing relative offset of tension before and after the perturbation as the cell density increases. Future experiments with varying cell density can easily test this.

In summary, the central result of this paper is that, on short time scales that preclude deposition and degradation of ECM, mechanical homeostasis on the tissue level likely results primarily from the contractile forces exerted by the cells on the surrounding tissue. Cells thereby re-establish a state only similar to the one prior to the perturbation. Using the mechanical analog model and computational framework presented in this paper to study the response of cell-seeded collagen gels and soft tissues to perturbations on longer time scales is a promising avenue of future research.

Declaration of Competing Interest

The authors declare that they have no known competing financial interests or personal relationships that could have appeared to influence the work reported in this paper.

Acknowledgments

This work was supported by the Deutsche Forschungsgemeinschaft (DFG, German Research Foundation) Projektnummer 257981274, Projektnummer 386349077. The authors gratefully acknowledge financial support by the International Graduate School of Science and Engineering (IGSSE) of Technical University of Munich, Germany. In addition, we thank Lydia Ehmer and Lea Haeusel for conducting some of the experiments and Isabella Jennings for advice and assistance with the experiments. We further gratefully thank Diane Tchibozo and Lisa Pretsch for contributing to Fig. 6A. Finally, we thank Abhay Ramachandra for his support in isolating the primary cells.

Supplementary material

Supplementary material associated with this article can be found, in the online version, at doi:10.1016/j.actbio.2021.07.054.

References

[1] J.J. Tomasek, G. Gabbiani, B. Hinz, C. Chaponnier, R.A. Brown, Myofibroblasts and mechano-regulation of connective tissue remodelling, Nat. Rev. Mol. Cell Biol. 3 (5) (2002) 349–363.
[2] J.D. Humphrey, E.R. Dufresne, M.A. Schwartz, Mechanotransduction and extracellular matrix homeostasis, Nat. Rev. Mol. Cell Biol. 15 (12) (2014) 802–812.
[3] G. Jiang, A.H. Huang, Y. Cai, M. Tanase, M.P. Sheetz, Rigidity sensing at the leading edge through $\alpha v\beta 3$ integrins and RPTPα, Biophys. J. 90 (5) (2006) 1804–1809.
[4] E.A. Cavalcanti-Adam, T. Volberg, A. Micoulet, H. Kessler, B. Geiger, J.P. Spatz, Cell spreading and focal adhesion dynamics are regulated by spacing of integrin ligands, Biophys. J. 92 (8) (2007) 2964–2974.
[5] D. Ben-Yaakov, R. Golkov, Y. Shokef, S.A. Safran, Response of adherent cells to mechanical perturbations of the surrounding matrix, Soft Matter 11 (7) (2015) 1412–1424.
[6] H. Wang, X. Xu, Continuum elastic models for force transmission in biopolymer gels, Soft Matter 16 (48) (2020) 10781–10808.
[7] M. Lerche, A. Elosegui-Artola, J.Z. Kechagia, C. Guzmán, M. Georgiadou, I. Andreu, D. Gullberg, P. Roca-Cusachs, E. Peuhu, J. Ivaska, Integrin binding dynamics modulate ligand-specific mechanosensing in mammary gland fibroblasts, iScience 23 (3) (2020) 100907.
[8] R.A. Brown, R. Prajapati, D.A. McGrouther, I.V. Yannas, M. Eastwood, Tensional homeostasis in dermal fibroblasts: mechanical responses to mechanical loading in three-dimensional substrates, J. Cell. Physiol. 175 (3) (1998) 323–332.
[9] J.D. Humphrey, Vascular adaptation and mechanical homeostasis at tissue, cellular, and sub-cellular levels, Cell Biochem. Biophys. 50 (2) (2008) 53–78.
[10] A.B. Kassam, M. Horowitz, Y.F. Chang, D. Peters, I.A. Awad, C.J. Hodge, G. Schackert, R.J. Dempsey, Altered arterial homeostasis and cerebral aneurysms: a molecular epidemiology study, Neurosurgery 54 (6) (2004) 1450–1460.
[11] J.D. Humphrey, D.M. Milewicz, G. Tellides, M.A. Schwartz, Dysfunctional mechanosensing in aneurysms, Science 344 (6183) (2014) 477–479.
[12] C.J. Cyron, J.D. Humphrey, Vascular homeostasis and the concept of mechanobiological stability, Int. J. Eng. Sci. 85 (2014) 203–223.
[13] Y. Yamashiro, H. Yanagisawa, The molecular mechanism of mechanotransduction in vascular homeostasis and disease, Clin. Sci. 134 (17) (2020) 2399–2418.
[14] V.M. Weaver, O.W. Petersen, F. Wang, C.A. Larabell, P. Briand, C. Damsky, M.J. Bissell, Reversion of the malignant phenotype of human breast cells in three-dimensional culture and in vivo by integrin blocking antibodies, J. Cell Biol. 137 (1) (1997) 231–245.
[15] D. Boettiger, D.A. Hammer, G.I. Rozenberg, K.R. Johnson, S.S. Margulies, V.M. Weaver, M. Dembo, C.A. Reinhart-King, A. Gefen, J.N. Lakins, N. Zahir, M.J. Paszek, Tensional homeostasis and the malignant phenotype, Cancer Cell 8 (3) (2005) 241–254.
[16] T. Yeung, P.C. Georges, L.A. Flanagan, B. Marg, M. Ortiz, M. Funaki, N. Zahir, W. Ming, V. Weaver, P.A. Janmey, Effects of substrate stiffness on cell morphology, cytoskeletal structure, and adhesion, Cell Motil. Cytoskeleton 60 (1) (2005) 24–34.
[17] K.R. Levental, H. Yu, L. Kass, J.N. Lakins, M. Egeblad, J.T. Erler, S.F. Fong, K. Csiszar, A. Giaccia, W. Weninger, M. Yamauchi, D.L. Gasser, V.M. Weaver, Matrix crosslinking forces tumor progression by enhancing integrin signaling, Cell 139 (5) (2009) 891–906.
[18] D.T. Butcher, T. Alliston, V.M. Weaver, A tense situation: forcing tumour progression, Nat. Rev. Cancer 9 (2) (2009) 108–122.
[19] P. Lu, V.M. Weaver, Z. Werb, The extracellular matrix: a dynamic niche in cancer progression, J. Cell Biol. 196 (4) (2012) 395–406.
[20] J. Kim, Y. Zheng, A.A. Alobaidi, H. Nan, J. Tian, Y. Jiao, B. Sun, Geometric dependence of 3d collective cancer invasion, Biophys. J. 118 (5) (2020) 1177–1182.
[21] J. Xie, M. Bao, S.M.C. Bruekers, W.T.S. Huck, Collagen gels with different fibrillar microarchitectures elicit different cellular responses, ACS Appl. Mater. Interfaces 9 (23) (2017). 1963, 0–19637.
[22] M.S. Hall, F. Alisafaei, E. Ban, X. Feng, C.-Y. Hui, V.B. Shenoy, M. Wu, Fibrous nonlinear elasticity enables positive mechanical feedback between cells and ECMs, Proc. Natl. Acad. Sci. 113 (49) (2016) 14043–14048.
[23] F. Grinnell, W.M. Petroll, Cell motility and mechanics in three-dimensional collagen matrices, Annu. Rev. Cell Dev. Biol. 26 (1) (2010) 335–361.
[24] M. Chiquet, L. Gelman, R. Lutz, S. Maier, From mechanotransduction to extracellular matrix gene expression in fibroblasts, Biochim. Biophys. Acta 1793 (5) (2009) 911–920.
[25] A. Mammoto, T. Mammoto, D.E. Ingber, Mechanosensitive mechanisms in transcriptional regulation, J. Cell Sci. 125 (13) (2012) 3061–3073.
[26] A. Zemel, Active mechanical coupling between the nucleus, cytoskeleton and the extracellular matrix, and the implications for perinuclear actomyosin organization, Soft Matter 11 (12) (2015) 2353–2363.
[27] R.C. Bates, L.F. Lincz, G.F. Burns, Involvement of integrins in cell survival, Cancer Metastasis Rev. 14 (3) (1995) 191–203.
[28] Y.K. Zhu, T. Umino, X.D. Liu, H.J. Wang, D.J. Romberger, J.R. Spurzem, S.I. Rennard, Contraction of fibroblast-containing collagen gels: initial collagen concentration regulates the degree of contraction and cell survival, Vitr. Cell. Dev. Biol. Anim. 37 (1) (2001) 10–16.
[29] S. Sukharev, F. Sachs, Molecular force transduction by ion channels — diversity and unifying principles, J. Cell Sci. 125 (13) (2012) 3075–3083.
[30] M.A. Schwartz, Integrins: emerging paradigms of signal transduction, Annu. Rev. Cell Dev. Biol. 11 (1) (1995) 549–599.

[31] J.D. Humphrey, Stress, strain, and mechanotransduction in cells, J. Biomech. Eng. 123 (6) (2001) 638–641.
[32] D.G. Ezra, J.S. Ellis, M. Beaconsfield, R. Collin, M. Bailly, Changes in fibroblast mechanostat set point and mechanosensitivity: an adaptive response to mechanical stress in floppy eyelid syndrome, Investig. Ophthalmol. Vis. Sci. 51 (8) (2010) 3853–3863.
[33] J.F. Eichinger, D. Paukner, J.M. Szafron, R.C. Aydin, J.D. Humphrey, C.J. Cyron, Computer-controlled biaxial bioreactor for investigating cell-mediated homeostasis in tissue equivalents, J. Biomech. Eng. 142 (7) (2020) 1–22.
[34] H. Wolinsky, S. Glagov, A lamellar unit of aortic medial structure and function in mammals, Circ. Res. 20 (1) (1967) 99–111.
[35] R.E. Shadwick, Mechanical design in arteries, J. Exp. Biol. 202 (Pt 23) (1999) 3305–3313.
[36] C. Zhu, C. Pérez-González, X. Trepat, Y. Chen, N. Castro, R. Oria, P. Roca-Cusachs, A. Elosegui-Artola, A. Kosmalska, Mechanical regulation of a molecular clutch defines force transmission and transduction in response to matrix rigidity, Nat. Cell Biol. 18 (5) (2016) 540–548.
[37] A. Elosegui-Artola, X. Trepat, P. Roca-Cusachs, Control of mechanotransduction by molecular clutch dynamics, Trends Cell Biol. 28 (5) (2018) 356–367.
[38] J.F. Eichinger, L.J. Haeusel, D. Paukner, R.C. Aydin, J.D. Humphrey, C.J. Cyron, Mechanical homeostasis in tissue equivalents - a review, Biomech. Model. Mechanobiol. 20 (3) (2021) 833–850.
[39] M. Marenzana, N. Wilson-Jones, V. Mudera, R.A. Brown, The origins and regulation of tissue tension: identification of collagen tension-fixation process in vitro, Exp. Cell Res. 312 (4) (2006) 423–433.
[40] R.A. Brown, K.K. Sethi, I. Gwanmesia, D. Raemdonck, M. Eastwood, V. Mudera, Enhanced fibroblast contraction of 3d collagen lattices and integrin expression by TGF-β1 and -β3: mechanoregulatory growth factors? Exp. Cell Res. 274 (2) (2002) 310–322.
[41] C. Courderot-Masuyer, Mechanical properties of fibroblasts, in: Agache's Measuring the Skin, Springer, 2017, pp. 903–909.
[42] B.H. Campbell, W.W. Clark, J.H.C. Wang, A multi-station culture force monitor system to study cellular contractility, J. Biomech. 36 (1) (2003) 137–140.
[43] A.H. Dahlmann-Noor, B. Martin-Martin, M. Eastwood, P.T. Khaw, M. Bailly, Dynamic protrusive cell behaviour generates force and drives early matrix contraction by fibroblasts, Exp. Cell Res. 313 (20) (2007) 4158–4169.
[44] D. Karamichos, R.A. Brown, V. Mudera, Collagen stiffness regulates cellular contraction and matrix remodeling gene expression, J. Biomed. Mater. Res. Part A 83 (3) (2007) 887–894.
[45] K.K. Sethi, I.V. Yannas, V. Mudera, M. Eastwood, C. McFarland, R.A. Brown, Evidence for sequential utilization of fibronectin, vitronectin, and collagen during fibroblast-mediated collagen contraction, Wound Repair Regen. 10 (6) (2002) 397–408.
[46] W.B. Cannon, Organization for physiological homeostasis, Physiol. Rev. IX (3) (1929) 399–431.
[47] D.D. Simon, L.E. Niklason, J.D. Humphrey, Tissue transglutaminase, not lysyl oxidase, dominates early calcium-dependent remodeling of fibroblast-populated collagen lattices, Cells Tissues Organs 200 (2) (2014) 104–117.
[48] T. Matsumoto, K. Hayashi, Mechanical and dimensional adaptation of rat aorta to hypertension, J. Biomech. Eng. 116 (3) (1994) 278–283.
[49] Y. Nakagawa, M. Totsuka, T. Sato, Y. Fukuda, K. Hirota, Effect of disuse on the ultrastructure of the achilles tendon in rats, Eur. J. Appl. Physiol. Occup. Physiol. 59 (3) (1989) 239–242.
[50] J.F. Eichinger, M.J. Grill, R.C. Aydin, W.A. Wall, J.D. Humphrey, C.J. Cyron, A computational framework for modeling cell-matrix interactions in soft biological tissues, Biomech. Model Mechanobiol. (2021).
[51] M.W. Majesky, Developmental basis of vascular smooth muscle diversity, Arterioscler. Thromb. Vasc. Biol. 27 (6) (2007) 1248–1258.
[52] Y.A. Miroshnikova, D.M. Jorgens, L. Spirio, M. Auer, A.L. Sarang-Sieminski, V.M. Weaver, Engineering strategies to recapitulate epithelial morphogenesis within synthetic three-dimensional extracellular matrix with tunable mechanical properties, Phys. Biol. 8 (2) (2011) 026013.
[53] J. Joshi, G. Mahajan, C.R. Kothapalli, Three-dimensional collagenous niche and azacytidine selectively promote time-dependent cardiomyogenesis from human bone marrow-derived MSC spheroids, Biotechnol. Bioeng. 115 (8) (2018) 2013–2026.
[54] I. Davoodi-Kermani, M. Schmitter, J.F. Eichinger, R.C. Aydin, C.J. Cyron, Computational study of the geometric properties governing the linear mechanical behavior of fiber networks, Comput. Mater. Sci. 199 (2021) 110711.
[55] J.A.J. Van Der Rijt, K.O. Van Der Werf, M.L. Bennink, P.J. Dijkstra, J. Feijen, Micromechanical testing of individual collagen fibrils, Macromol. Biosci. 6 (9) (2006) 699–702.
[56] K.A. Jansen, A.J. Licup, A. Sharma, R. Rens, F.C. MacKintosh, G.H. Koenderink, The role of network architecture in collagen mechanics, Biophys. J. 114 (11) (2018) 2665–2678.
[57] W. Chen, J. Lou, E.A. Evans, C. Zhu, Observing force-regulated conformational changes and ligand dissociation from a single integrin on cells, J. Cell Biol. 199 (3) (2012) 497–512.
[58] F. Kong, A.J. García, A.P. Mould, M.J. Humphries, C. Zhu, Demonstration of catch bonds between an integrin and its ligand, J. Cell Biol. 185 (7) (2009) 1275–1284.
[59] D. Choquet, D.P. Felsenfeld, M.P. Sheetz, N. Carolina, Extracellular matrix rigidity causes strengthening of integrin cytoskeleton linkages, Cell 88 (1) (1997) 39–48.
[60] S.W. Moore, P. Roca-Cusachs, M.P. Sheetz, Stretchy proteins on stretchy substrates: the important elements of integrin-mediated rigidity sensing, Dev. Cell 19 (2) (2010) 194–206.
[61] S.J. Stehbens, T. Wittmann, Analysis of focal adhesion turnover: a quantitative live-cell imaging example, Methods Cell Biol. 123 (2014) 335–346.
[62] BACI: A Comprehensive Multi-Physics Simulation Framework 2021. https://baci.pages.gitlab.lrz.de/website (Accessed June 23, 2021).
[63] R. Nissen, G.J. Cardinale, S. Udenfriend, Increased turnover of arterial collagen in hypertensive rats, Proc. Natl. Acad. Sci. 75 (1) (1978) 451–453.
[64] E. Gineyts, P.A. Cloos, O. Borel, L. Grimaud, P.D. Delmas, P. Garnero, Racemization and isomerization of type i collagen c-telopeptides in human bone and soft tissues: assessment of tissue turnover, Biochem. J. 345 (Pt 3) (2000) 481–485.
[65] S.M. Hall, A. Soueid, T. Smith, R.A. Brown, S.G. Haworth, V. Mudera, Spatial differences of cellular origins and in vivo hypoxia modify contractile properties of pulmonary artery smooth muscle cells: lessons for arterial tissue engineering, J. Tissue Eng. Regen. Med. 1 (4) (2007) 287–295.
[66] D.D. Simon, L.O. Horgan, J.D. Humphrey, Mechanical restrictions on biological responses by adherent cells within collagen gels, J. Mech. Behav. Biomed. Mater. 14 (2012) 216–226.
[67] S. Weng, Y. Shao, W. Chen, J. Fu, Mechanosensitive subcellular rheostasis drives emergent single-cell mechanical homeostasis, Nat. Mater. 15 (9) (2016) 961–967.
[68] M. Hippler, K. Weißenbruch, K. Richler, E.D. Lemma, M. Nakahata, B. Richter, C. Barner-kowollik, Y. Takashima, A. Harada, E. Blasco, M. Wegener, M. Tanaka, M. Bastmeyer, Mechanical stimulation of single cells by reversible host-guest interactions in 3d microscaffolds, Sci. Adv. 6 (39) (2020) eabc2648.
[69] K.D. Webster, W.P. Ng, D.A. Fletcher, Tensional homeostasis in single fibroblasts, Biophys. J. 107 (1) (2014) 146–155.